

Compact Object Formation and the Supernova Explosion Engine

Chris L. Fryer

CCS-2, MS D409, Los Alamos National Laboratory Los Alamos, NM, 87544

E-mail: fryer@lanl.gov

Abstract.

When a massive star ends its life, its core collapses, forming a neutron star or black hole and producing some of the most energetic explosions in the universe. Core-collapse supernovae and long-duration gamma-ray bursts are the violent signatures of compact remnant formation. As such, both fields are intertwined and, coupled with theory, observations of transients can help us better understand compact remnants just as neutron star and black hole observations can constrain the supernova and gamma-ray burst engine. We review these ties in this paper.

1. The progenitors of Compact Remnants

In molecular clouds, clumps of gas can become gravitationally bound and contract. Ultimately, the compressing gas heats up sufficiently to drive the fusion of hydrogen into helium and the birth of a star. For most of its life, hydrogen fusion powers the star (the so-called main sequence evolution). Ultimately, the hydrogen is depleted in the core and the star expands into a giant phase as its core contracts. For massive stars, this phase represents just the first in a series of burning phases where the ashes of the first phase ignite as the core contracts: core contraction continues until helium fusion occurs, a second core contraction until the products of helium fusion (carbon, oxygen) ignite, and so on until an iron core is built in the center of the star. Silicon shell burning above the iron core continues to increase its mass until the thermal and electron degeneracy pressure in the core is no longer able to support its mass and the core collapses.

The collapse of these cores produce most of the stellar-massed neutron stars (NSs) and black holes (BHs) in the universe[‡]. The energy released in these core collapses produce supernovae (type Ib/c and II) and long-duration gamma-ray bursts (GRBs). The nature and mass of the remnants is directly connected to the nature of the explosion. In this paper, we review the current models for the explosions from stellar implosion and the resultant role they play on the compact remnants produced in the implosion. Section 2 reviews the current explosion mechanisms and section 3 reviews how these explosions dictate the remnant mass distribution. These sections cover theoretical expectations. We conclude with a discussion of the current observations including the expectations from gravitational wave detections.

2. Explosions from Stellar Collapse

2.1. Convection-Enhanced Supernovae

As the iron core collapses, the subsequent higher densities and temperatures drive further dissociation of the iron in the core (removing thermal support) and increased electron capture (removing electron degeneracy support) causing the collapse to accelerate. Ultimately, the core collapses at over 1/10th the speed of light. This nearly free-fall collapse continues until the core reaches nuclear densities, where nuclear forces and neutron degeneracy halt the collapse, producing a proto-neutron star (PNS)[§]. At this time, a roughly $0.8\text{-}1.0 M_{\odot}$ iron core has collapsed from ~ 5000 km down to 50 km. The sudden halt of the collapse causes the infalling material to “bounce”.

[‡] A subset of neutron stars are produced by the collapse of ONe cores that collapse before creating an iron core - the so-called electron capture supernovae. In a similar manner accreting ONe white dwarfs can collapse if they accrete enough material in an interacting binary. The collapse of these systems is similar to the iron cores, and we will focus on the iron core collapse scenario in this review.

[§] As we shall discuss in Section 2.3, the high entropy cores of very massive stars, the collapse halts before reaching nuclear densities and the core can collapse to a BH prior to reaching nuclear densities.

In the collapse, roughly $GM_{\text{PNS}}^2/R_{\text{PNS}} \approx 10^{53}$ erg \parallel of gravitational potential energy is released (far above what is needed to power typical supernovae). Unfortunately, converting just 1% of this energy into explosion energy to make a 10^{51} erg supernovae \P has proven extremely difficult. The first simulations argued that the “bounce” would convert the potential energy released into outward-moving kinetic energy, driving an explosion [1]. However, much of the energy in this bounce is stored in thermal/neutrino energy and when neutrino transport is included, the bounce explosion stalls as soon as the neutrinos are no longer trapped in the shock (roughly at 100-200 km).

Over the past 40-50 years, astrophysicists have focused on studying how to revive this shock. The rest of the star falls onto the stalled shock and the ram pressure of this infalling material must be overcome to drive a successful explosion. Both a region within the PNS and the region between the PNS and the stalled shock are susceptible to a number of convective instabilities $^+$. These instabilities can increase the efficiency at which the potential energy is converted into explosion energy to revive the shock and blow off the infalling star. Much of the current work is focusing on the interplay of the enhancement in energy conversion from convection coupled to the increasingly complex physics needed to model core collapse (behavior of matter at extreme densities, neutrino emission and cross-section, neutrino transport, and magnetic fields).

Most of the current work is focused on the convection between the PNS and the stalled shock [2], where turbulence is able to extract energy released near the surface of the NS and convert it to kinetic energy driving out the shock (see Figure 1). The energy in the convective region must overcome the ram pressure of the infalling star. This ram pressure (P_{shock}) of the infalling material rapidly decreases with radius ($P_{\text{shock}} \propto \rho v^2 \propto r^{-3} - r^{-4}$ [4]), so if the stalled shock can be forced outward, it will quickly accelerate, launching an explosion. Our current focus is on understanding the nature of the turbulence (e.g. whether it is driven by Rayleigh Taylor or standing accretion shock instabilities), the source of the energy (hot proto-neutron star, PNS oscillations, pressure waves from material accreting onto the PNS) and what critical physics is missing in the current models (e.g. neutrino interactions and transport, equation of state, magnetic fields). All these topics remain areas of intense debate. Fueled by the fact that GRBs and hypernovae are almost certainly driven by a different mechanism, many astronomers are studying mechanisms beyond this convection-enhanced engine.

Before we discuss these alternate mechanisms, let’s study in more detail some of the scenarios within the convection-enhanced engine paradigm using figure 1 as a guide. After the collapse and bounce, unless there are significant pathologies in the equation of state, the entropy profile from the PNS out to the shock will decrease ($\partial S/\partial r < 0$ [3, 4]

\parallel In this equation, G is the gravitational constant, M_{PNS} is the mass of the core (1-1.4 M_{\odot}) and R_{PNS} is the radius of the collapsed core (typically this radius is initially 50 km but as the PNS cools, it contracts to 10 km).

\P Hans Bethe termed this unit a “foe” for **fifty one erg**, but it has also been termed a “Bethe”.

$^+$ Here, we define convection as any instability driving mass motions within a region, similar to the terminology used in stellar evolution.

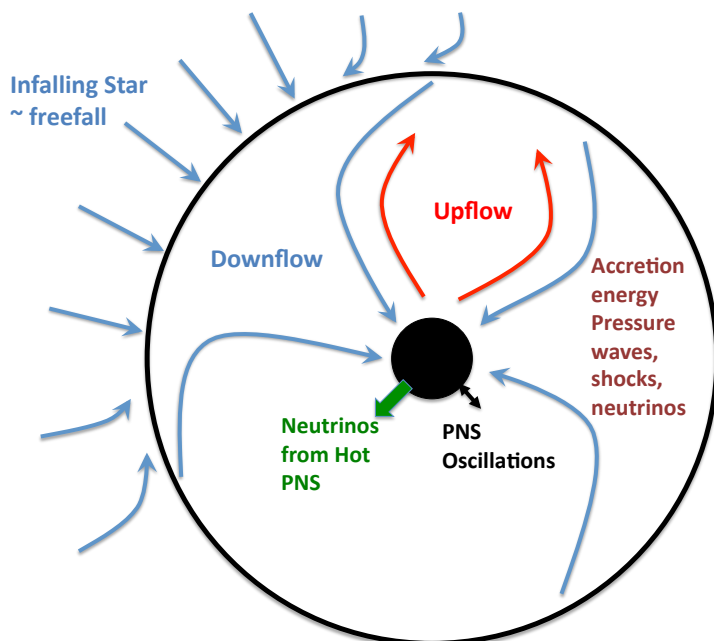


Figure 1. Diagram of the supernova engine. The collapsed core forms a PNS roughly 50 km in size. The bounce shock moves outward to 100-200 km before stalling. At this point, the rest of the star has realized its core has collapsed and falls onto this stalled shock. That material builds on the stalled shock, flowing to low points. After enough matter is built up, it sends downflows toward the PNS. Material heated by a range of energy sources (neutrinos leaking out of the PNS or from accreting material, shocks on the PNS surface, PNS oscillations) rises in bubbles, converting the heat energy into kinetic energy that pushes out on the stalled shock. If this energy can overcome the ram pressure of the infalling star, the stalled shock can move outward and drive an explosion.

and such a profile is unstable to Rayleigh-Taylor instabilities[5, 2]. The growth time of such instabilities is roughly a few milliseconds[6] and we expect Rayleigh-Taylor to dominate at early times. Much of the potential energy released in the collapse of the core is converted into heat in the PNS and this heat leaks out of this star via neutrinos. These neutrinos heat material just above the PNS, further increasing the entropy gradient to drive further Rayleigh-Taylor convection. The neutrino-deposited energy is converted into kinetic energy as the hot bubbles rise from the PNS base, pushing against the infalling star. This convective engine is depicted in a slice of a 3-dimensional calculation in figure 2. As the collapsing star piles up on the stalled shock, it flows toward low points, piling up until a downflow is produced. The low entropy material flows down onto the PNS, producing shocks and enhancing the neutrino emission (contributing additional sources of energy). If the energy is sufficient to drive the shocked region

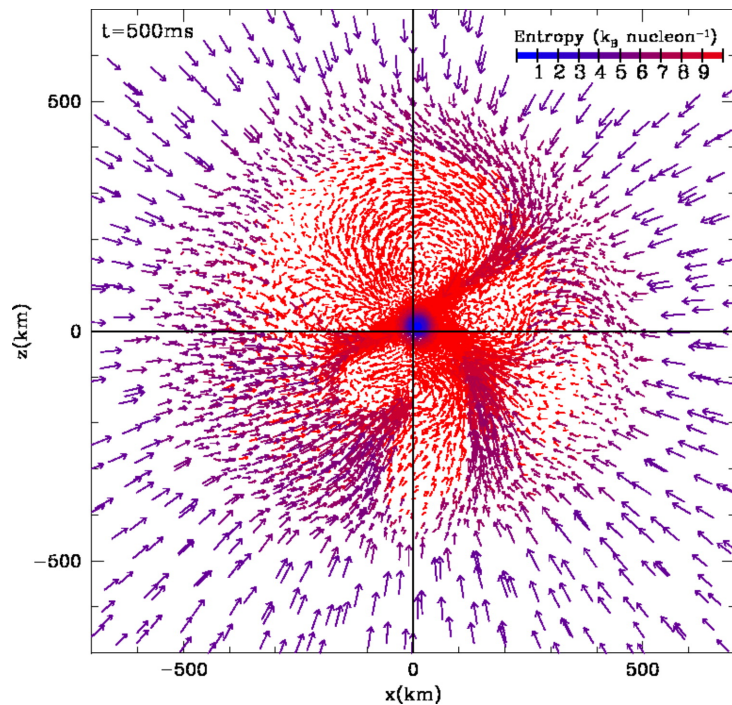


Figure 2. Slice in the x - z plane of a 3-dimensional core-collapse simulation[6]. The shading denotes entropy and the arrows denote velocity direction and magnitude. As the star implodes, the outer layers of the star rain down on the collapsed core and flow around the upflows to form downflows. The downflows crash onto the PNS, adding to the neutrino emission. Shock energy also can increase the entropy of the material, contributing to upflows.

outward, the ram pressure will quickly decrease, allowing a strong supernova explosion. As the explosion becomes strong, the convective engine turns off. In this way, the amount of energy in the explosion can be estimated by setting it equal to the energy stored in the convective region when the ram-pressure lid is blown off, allowing us to calculate fallback and final remnant masses (Sec. 3).

Rayleigh-Taylor convection should occur in all simulations of stellar collapse. Indeed, calculations that don't exhibit Rayleigh-Taylor convection typically either have some pathology in their equation of state preventing a large initial entropy gradient, their resolution is too low and numerical viscosity prevents the growth of the Rayleigh-Taylor instability, or their initial conditions are post-bounce and do not include an entropy gradient. All calculations suffer from low-resolution, explaining why, except in a few cases, the Rayleigh-Taylor growth in the simulations is typically ten times longer than the analytic predictions. If the Rayleigh-Taylor convection can quickly reset the entropy profile, other instabilities can develop[7]*. It is this assumption that forms the basis for the standing accretion shock instability[8, 9]. In this scenario, entropy/vorticity perturbations are advected downward in the flow and couple with acoustic perturbations.

* Note, however that simulations of this profile show that such a resetting of the entropy profile takes longer than the 10 or so turnover times expected in rapid accretion onto NSs[6].

This instability can drive low-mode oscillations, again converting potential energy released near the base of the PNS into kinetic energy at the edge of the stalled shock. Like the Rayleigh-Taylor instability, the energy in this explosion can be estimated by the maximum energy stored in the convective region.

All in all, scientists have focused on a few variants in instabilities:

- Rayleigh-Taylor Instability: driven by entropy gradients, high-entropy (or “hot”) bubbles will rise from the PNS surface. Low entropy material will find low points in the stalled shock, pile up, and form downstreams[10, 11, 2].
- Rotationally stabilized Rayleigh-Taylor, also known as the Solberg-Høiland instability[12]: if the specific angular momentum increases as one moves outward in radius (typical for rotating massive star structures), the angular momentum profile will stabilize against convection. This can produce asymmetric explosions[13].
- Composition gradients and Rayleigh-Taylor: Composition gradients, e.g. gradients in the electron fraction in the PNS core can drive or stabilize against convection (if it counters the entropy gradient, the relative diffusion of heat and composition can drive a doubly diffusive instability). This instability is studied primarily in convection within the PNS[14, 15].
- Acoustic/Advective Instability (the standing accretion shock instability is a variant of this instability): This instability, coupling vorticity and pressure waves, is slower to grow than Rayleigh-Taylor but may develop and dominate in some scenarios[8, 9, 16].

and a range of energy sources:

- Thermal energy in the PNS: (gravitational potential energy released in initial collapse). The energy is radiated from the NS in the form of neutrinos[17].
- Gravitational energy released from infalling material striking the PNS. Shocked material may drive some material to rise or neutrinos from the accreting material can transfer energy.
- PNS oscillations: The accretion, especially in acoustic/advective instabilities, can drive oscillations in the NS[18], although see[6, 19].
- Rotational Energy: If the star is rotating rapidly, a disk can form around the PNS. This rotational energy can drive a dynamo that generates strong magnetic fields to drive an explosion[20, 21]. The rotation period during the engine for even the fastest-spinning stars is typically too long (70-770 ms) to wind a strong magnetic field during the initial engine, but as the PNS contracts, this engine becomes viable[13, 22].

2.2. Late-Time Energy Sources

As the convective region expands with the launch of the explosion, the amount of mass in this region that can absorb neutrinos from the hot PNS decreases, effectively shutting

off this source of energy. PNS oscillations can deposit energy longer, but even this energy source diminishes. However, new energy sources develop after the collapse. Both post-explosion fallback and rotational energy have been invoked to drive explosions.

Supernova “fallback” is material initially ejected in the supernova explosion that ultimately falls back onto the PNS. Two major scenarios have been proposed to explain this fallback focusing on a 1-dimensional picture of supernova explosions. The first argued that the ejecta decelerates as it plows through the imploding star. It produces an explosion, but loses enough energy to fall back onto the PNS[23]. Alternatively, a reverse shock is produced when the supernova shock enters the hydrogen envelope (with its shallow density gradient). This reverse shock drives fallback[24]. The primary difference between these two scenarios is that the reverse shock scenario only produces fallback after a considerable delay (the shock must first reach the hydrogen envelope and then the reverse shock must decelerate the outward moving material causing it to fall back). The ejecta deceleration model[23] tends to produce considerable fallback in the first 1-15 s[30].

The amount and nature of then fallback in 1-dimensional simulations depends not just on the characteristics of the explosion (progenitor star and explosion energy), but also on the numerical implementation of the explosion [25, 26, 27, 30, 28, 29]. Indeed, those models using piston-driven explosions are limited to the late-time reverse-shock fallback. Energy injected models have more fallback primarily in the first 1-15 s after the launch of the explosion [30] (for a comparison of these two engines, see [26]). In multi-dimensional simulations, fallback occurs even as the shock is launched as low-entropy material flows down through the hot rising shock. This is seen both in late-time explosion calculations and ejecta supernova explosions, making it difficult to distinguish fallback from the supernova mechanism itself [41, 42]. For this paper, we will call any material accreting onto the NS after the launch of the shock “fallback”. This fallback shocks when it hits the cooling PNS and some of the material is re-ejected in plumes (Fig. 3) [4, 30]. These plumes can make up a sizable fraction of the explosion energy, especially in those weak explosions that produce considerable fallback. The amount of fallback ties the nature of the explosion engine directly to the remnant mass. We will discuss fallback in much greater detail in section 3.

Rotating stars produce asymmetric explosions that tend to leave behind disks around the PNS. Magnetic fields are capable of extracting this rotation energy to drive a second explosion. After the launch of the explosion, the PNS contracts. Any rotation disk will contract, speeding its rotation period and within a few seconds a dynamo can create a strong magnetic field. This magnetic field may produce jet-like explosions with a NS compact remnant[22].

The inner core of a massive star often couples to outer layers, causing its angular velocity to be on par with these outer layers. This means the core’s angular momentum is quite low. If, however, the PNS collapses to a BH and the inner $3-5M_{\odot}$ accretes onto the compact remnant, the higher angular momentum material of the outer core can form a rapidly spinning accretion disk around the black hole. It is this disk that has been

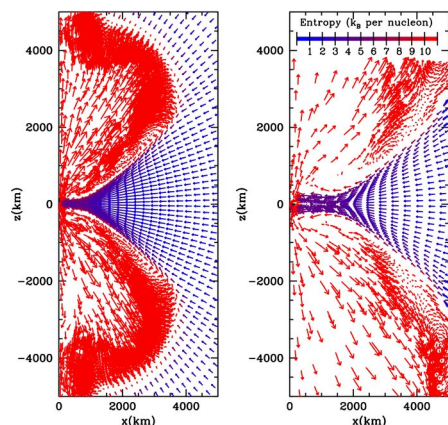


Figure 3. An x-z image of a 2-dimensional simulation of outflows from fallback. The vectors dictate the direction and magnitude of the velocity and the shading denotes the entropy. Some of the material receives enough entropy to rise and escape the downflow. The initial accretion rate is $0.01M_{\odot} \text{ s}^{-1}$ and there is a modest amount of angular momentum ($3 \times 10^{15} \text{ cm}^2 \text{ s}^{-1}$) that provides a preferred ejection direction (along the rotation axis).

invoked to form the collapsar GRB engine [31, 32]. The collapsar model argues that a magnetic dynamo in the disk (or neutrinos in the disk) produce a highly-relativistic jet, producing a gamma-ray burst. This jet eventually disrupts the star, halting accretion and limiting the black hole mass.

2.3. Very Massive Stars

As the mass of the star increases, a new instability can occur whereby pair-creation in the core causes the star to collapse and undergo explosive oxygen and silicon burning[33, 34, 35, 36]. For stars with masses above $\sim 260M_{\odot}$, a sufficiently large fraction of the center of the star becomes so hot that photodisintegration occurs before explosive burning reverses the implosion, accelerating the collapse[35]. These high entropy cores halt the infall before reaching nuclear densities, forming a proto-BH and producing a very different neutrino signal from lower mass stars and produce, at best, a disk wind outburst much dimmer than any supernova[37]. The proto-BH keeps accreting until an event horizon forms around it. Such proto-BH persists out to masses above $100,000M_{\odot}$ [38] and the fate can only be altered if the core is rapidly rotating.

3. Black Hole Formation and Masses

There are 3 basic ways a BH forms in stellar collapse.

- Direct Collapse: In systems where all the explosion mechanisms discuss in section 2.1 fail to revive the shock, the PNS continues to accrete and ultimately becomes too massive to support itself, collapsing to form a BH. In these systems, the mass of the BH is the mass of the star at collapse. Fryer[43, 44] argued that

stars above $\sim 40M_{\odot}$ (neglecting mass loss from winds and binary interactions) collapse directly to BHs. More recent estimates predict a lower limit but with large variations caused by stellar mass loss[43].

- **Fallback Collapse:** In systems where a weak explosion occurs, much of the material initially ejected at the launch of the explosion falls back, causing the PNS to collapse to a BH [43]. This formation scenario can form a wide range of masses for low-mass BHs.
- **Proto-BH Formation:** Very massive stars (above $\sim 300M_{\odot}$) produce a proto-BH that accretes mass until an event horizon forms, causing it to become a true black hole[37]. Like the direct collapse stars, these stars form BH masses set to the stellar mass at collapse.

Most “normal” supernovae have explosion energies between $1 - 3 \times 10^{51}$ erg, only 1% of the total potential energy released in the collapse. The convective engine provides a natural explanation for this 1% efficiency: because energy deposition drops as soon as the shock is launched, the explosion energy is set to the energy stored in the convective region prior to the launch of the shock (see[39] for more details). In this manner, the explosion energy depends upon the ram pressure from the infalling stellar material; a function of both the stellar progenitor and the time of explosion. Figure 4 shows the explosion energies as a function of explosion times for 3 progenitor masses (assuming no mass loss). The maximum energy stored in the convective engine is never more than a few times 10^{51} erg, explaining why the energy in normal supernovae are only 1% the total energy released‡. These strong explosions have very little fallback (less than a few tenths of a solar mass) and the remnants are typically NSs.

Although this naturally explains most supernovae, if the explosion is delayed (taking more than 100ms after bounce), explosion energies are typically less than 10^{51} erg. These weaker explosions lead to considerable fallback, producing a range of remnant masses from massive NSs ($2M_{\odot}$) to BHs with masses nearly as massive as those produced through “direct” collapse. Supernovae with considerable fallback provide a unique probe into the supernova engine. Figure 5 shows the mass of the fallback material as a function of time for multiple explosion energies and 3 different stellar progenitor masses. Most of the fallback happens in the first 1-15s after the launch of the shock††. Above $\sim 20M_{\odot}$, the explosion energy must be very strong to avoid significant fallback. For example, a 2×10^{51} erg (2 foe) explosion for our binary $23M_{\odot}$ progenitor has over $1.1M_{\odot}$ of fallback in the first 15s.

The cumulative distribution of remnant masses for both delayed and rapid engine models for 3 different metallicities is shown in figure 6. In these models, 80-90% of all compact remnants are NSs. For the rapid explosions, 75-95% of these NSs have

‡ Hypernove and GRBs can extract up to 10% the total energy released, clearly requiring a different/additional energy source beyond the convective engine.

†† This means that any additional energy from fallback will be able to catch up to the shock before the shock breaks out of the star, contributing to the observed supernova explosion energy. This may be alternate explanation for bright supernovae with low ^{56}Ni , e.g. SN 2005bf[40].

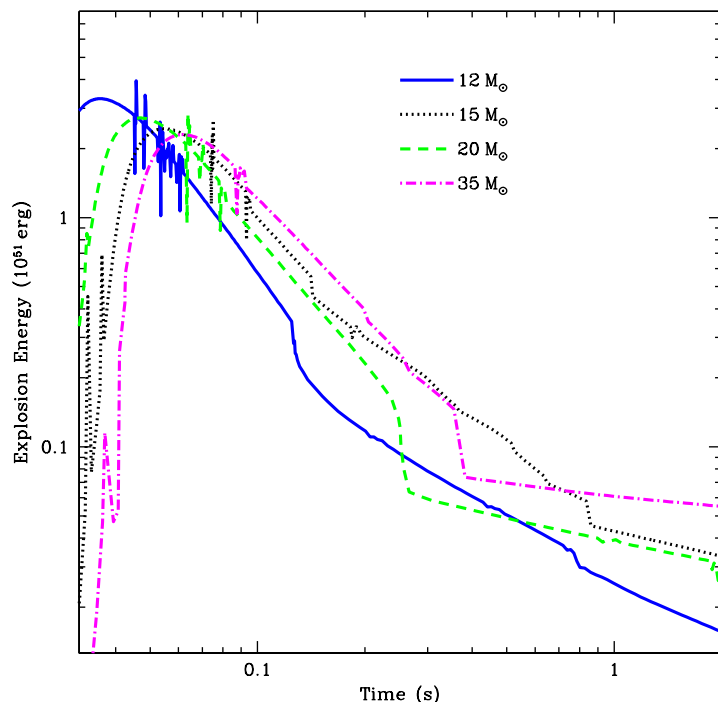


Figure 4. Supernova explosion energy as a function of the time it takes, post-bounce, for the shock to be revived [39]. The density drops rapidly in the star as one moves from the silicon core through the carbon/oxygen and helium layers. This drop in density converts to a drop in mass infall rate (\dot{M}) when the star implodes. The total energy stored is proportional to the ram pressure (P_{ram}) that, in turn, is set by the mass infall rate: $P_{\text{ram}} = 1/2\rho_{\text{infall}}v_{\text{infall}}^2 = (\dot{M}v_{\text{infall}})/(8\pi r_{\text{shock}}^2)$ where ρ_{infall} and v_{infall} are, respectively, the infall density and velocity and r_{shock} is the radius of the stalled shock. As the carbon/oxygen shell becomes the dominant infalling material, the pressure drops considerably. If the convective engine has stored up 10^{51} erg of energy in the turbulent region, it will explode. After this time, the maximum energy that can be stored in the convective region is well below the typical 1 – 3foe/Bethe supernova energy (see[39] for more details).

masses below $1.6M_{\odot}$. Very few remnants are produced with masses between $2M_{\odot}$ and $4M_{\odot}$. For the delayed explosion, a more distributed range of masses exist. With these differences, accurate observations of the mass distribution will determine whether a rapid or delayed explosion dominates the supernova engine (shedding light into the convective instability) and whether a new energy source is needed beyond that available in the convective region.

3.1. Compact Remnant Kicks

Most observations of compact remnants are focused on compact remnants in binaries. Binary observations are a biased sample, limited to those systems that remain bound after the formation of the compact binary. The violent collapse of a stellar core can

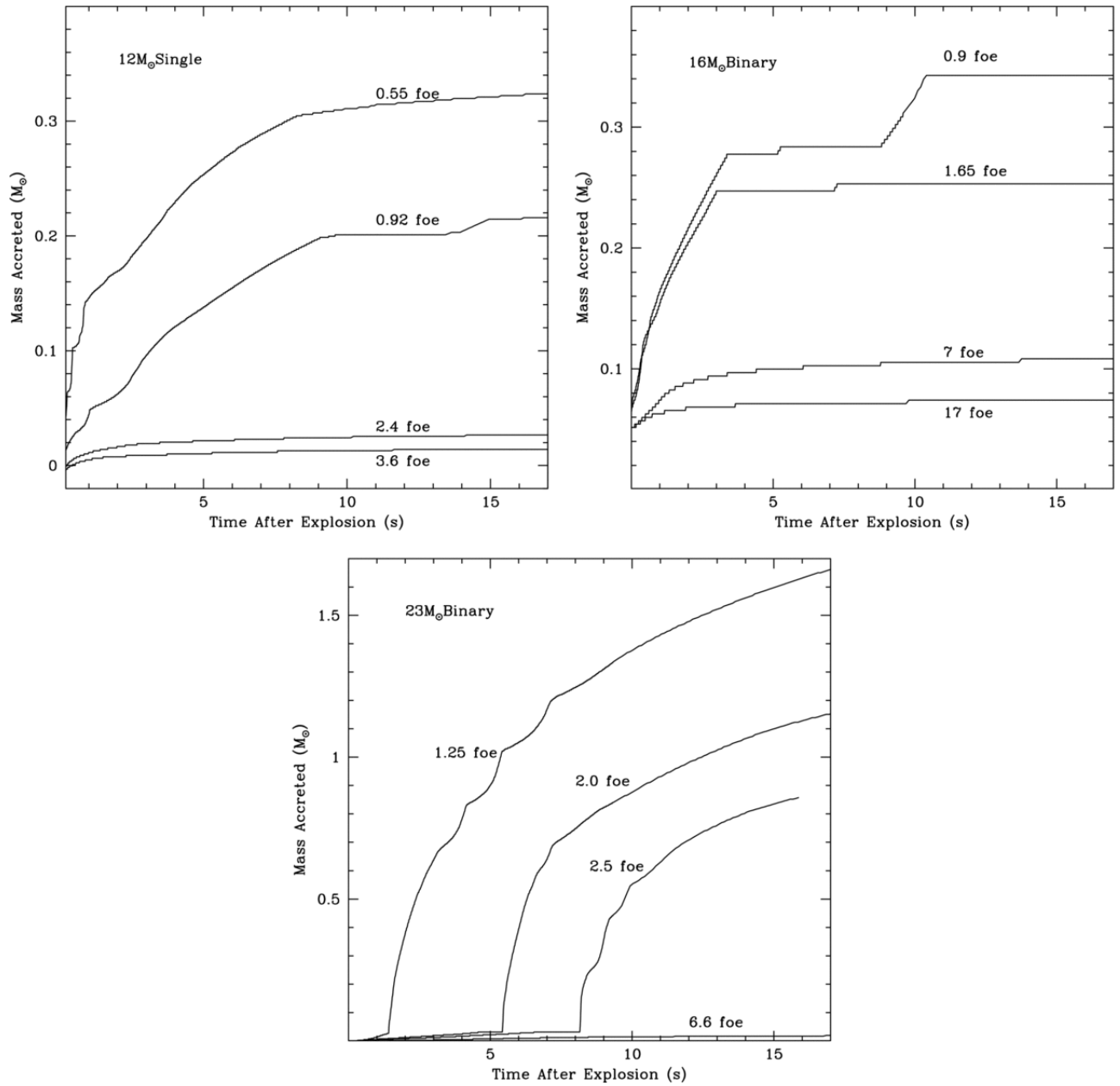


Figure 5. Amount of fallback for 3 different progenitors: $12M_{\odot}$ single star and $16M_{\odot}$ and $23M_{\odot}$ binary stars (in the binary systems, the hydrogen is removed during a common envelope evolution phase, removing reducing the mass)[30]. Note that the fallback begins within the first second and most occurs within the first 15s. For stars with masses above $20M_{\odot}$, there is considerable fallback (more than $0.5M_{\odot}$) for any explosion with normal (1-3foe) explosion energies.

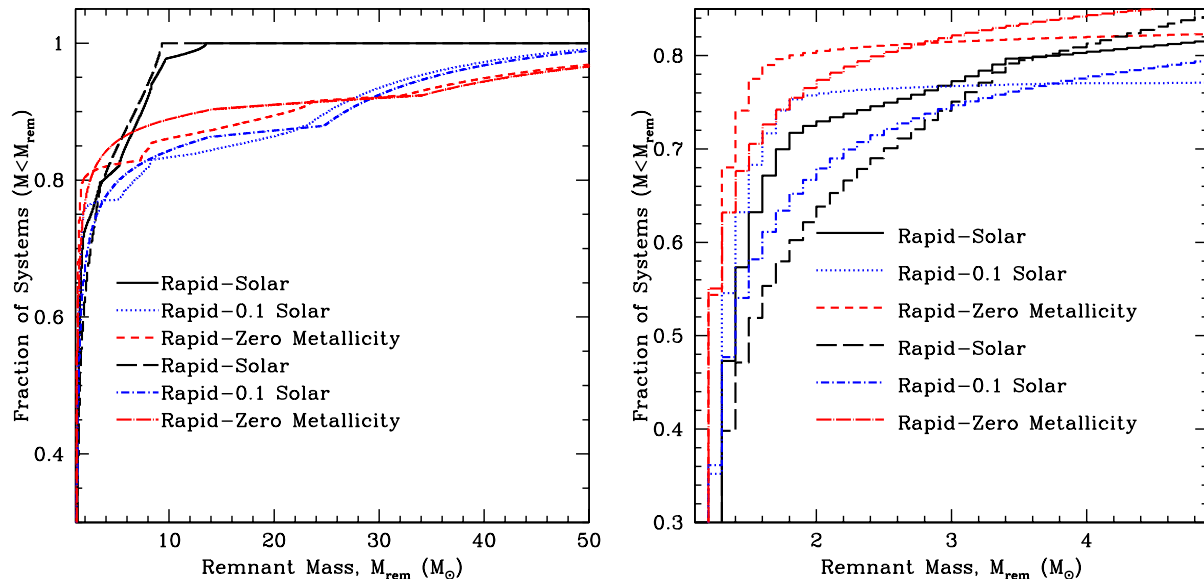


Figure 6. Cumulative fraction of remnant masses as a function of mass for 6 models: 3 rapid and 3 delayed explosions each at solar, 0.1 solar and zero Metallicity. In these models, 80-90% of all compact remnants are NSs. For the rapid explosions, 75-95% of these NSs have masses below $1.6M_{\odot}$. Very few remnants are produced with masses between $2M_{\odot}$ and $4M_{\odot}$. For the delayed explosion, a more distributed range of masses exist.

impart large velocities on the compact remnants. To understand these systems, we must understand the “kicks” imparted on these remnants at birth.

A growing set of both NS and BH binaries seem to require that the compact remnant receive a burst of momentum at formation[45, 46, 47, 48, 49]. Observations of pulsar proper motions suggest that the distribution of these kicks contains a sizable fraction of neutrons stars moving with velocities in excess of 400km s^{-1} [50, 51]. Although uncertainties persist in these measurements (distance errors, issues such as biases in the sampling - systems with stronger kicks are more likely to escape the galaxy), these observations place fairly strong constraints on kicks received by NSs. Much less is known about the BH kick distributions; aside from a few binaries that suggest kicks are needed for some systems, we have very little information on BH kicks[48, 49].

Although there exist many theories to explain kicks, nearly all have trouble explaining those pulsars with velocities in excess of 1000km s^{-1} and although there is a preference among theorists towards kicks produced by asymmetries in the supernova ejecta, no kick mechanism can truly be ruled out or in. Most of the kick mechanisms invoke asymmetries in the supernova explosion whereby momentum conservation requires that if the ejecta is driven preferentially in one direction, the compact remnant must be directed in the opposite direction with equal momentum. This means that both the mass and velocity of the ejecta asymmetry is critical. In this way, GRB jets have difficulties driving kicks. With only $\sim 10^{-6}M_{\odot}$ in the jet mass, even if the jet is

one-sided with a lorentz factor of 500, the kick on a $5M_{\odot}$ BH is only 30km s^{-1} . But a number of both ejecta and neutrino asymmetries could produce large kicks:

- Binary disruption: The sudden ejection of the supernova can disrupt a binary star system. If the supernova has a lot of ejecta and the binary is close, this scenario produces kicks up to 200km s^{-1} , well below the bulk of the pulsar velocities[52]. The ejecta in a binary can also impart bulk velocities on the bound binaries, but these velocities are extremely low and can not explain the fastest binary systems[48, 49].
- Propeller: Asymmetric emission of radio waves for pulsars where the magnetic field is off-centered and inclined to the axis of rotation[53].
- Growth of Pre-Collapse Asymmetries: Although it has been argued that asymmetries in the initial structure could drive strong kicks, realistic calculations show that only abnormally large asymmetries can produce kicks above a few hundred km s^{-1} [54].
- Low-Mode Rayleigh Taylor: As the Rayleigh-Taylor instability develops, the lowest modes grow roughly to the size of the stalled shock (Fig. 2). Such low modes can drive asymmetries in the supernova explosion ejecta, producing kicks[55]. This mechanism has received some success[56].
- Advective/Acoustic Instabilities: Low-mode instabilities are characteristic in this instability and several groups have studied the kicks from these instabilities[].
- Neutrino Asymmetry from Neutrinosphere Turbulence: Magnetoacoustic instabilities producing neutrino bubbles akin to the photon bubble instability produces asymmetric neutrino emission as the neutrino bubbles rise to the neutrinosphere[57].
- Neutrino Oscillations: If the core has extremely strong magnetic fields, neutrino oscillations coupled to those magnetic fields, can produce strong neutrino asymmetries[58, 59, 60, 61, 62, 63, 64].

Unfortunately, none of these kick mechanisms are well-enough understood to then infer kick distributions for BHs. But the kick placed on the BH can be categorized into 3 fates[65]:

- No Kick: the propeller mechanism for all BHs, binary disruption and all ejecta explosions for direct BHs, neutrino-driven kicks may work in all BH formation scenarios.
- Equal Momentum Kicks: Binary and ejecta-driven kick mechanisms are likely to produce kicks with equal momenta to their NS counterparts, hence the kick velocity is roughly $\propto M_{\text{NS}}/M_{\text{BH}} \times v_{\text{NSkick}}$ where M_{NS} , M_{BH} are the NS, BH masses respectively and v_{NSkick} is the NS velocity (taken from the proper motion studies of pulsars. For neutrino driven mechanisms, this case may hold for both fallback and direct collapse BH scenarios.
- Enhanced Momentum Kicks: For convective-instability kick mechanisms, asymmetries are strongest in delayed explosions, exactly those explosions that produce a lot of fallback. These systems might get the strongest kicks.

For BH kicks, a few scenarios are typically implemented into population studies of binary BH systems: BHs receive no kicks whatsoever (there is a growing belief that this is disproved by observations - e.g.[48, 49]), all BHs receive kicks with conserved momentum: $v_{\text{kick}} \propto M_{\text{NS}}/M_{\text{BH}} \times v_{\text{NSkick}}$, direct BHs receive no kicks and BHs with fallback receive kicks (either with conserved momentum, or in the enhanced case, with the same velocity as the pulsar observations). If one of these can be demonstrated absolutely, we would have constraints on the kick mechanism for both NSs and BHs. In addition, these kick distributions must be understood to tie theoretical mass distributions to observations of binary systems.

4. Observational Constraints: Supernovae and Compact Remnant Masses

Currently, the primary constraints on the mass distributions of compact remnants is limited to binaries containing NSs and BHs (e.g. X-ray binaries and binary pulsars). Early analyses of these binaries suggested that NS masses clustered with a very narrow mass range around $1.35 \pm 0.04 M_{\odot}$ [66] and BHs clustered with a broader range ($\sim 1 M_{\odot}$) around $7 M_{\odot}$ [67]. But as new systems have been added and the data on existing systems has become more refined, it has become clear that the distribution of NSs is more spread out with neutron star masses ranging from $\sim 1.1 M_{\odot}$ [68] to $\sim 2 M_{\odot}$ [69]. BH mass measurements are even more difficult to make, relying upon a complex combination of both observations of X-ray binaries and modeling of photometric and spectroscopic data. Although the BH mass range has widened with time, one aspect of the mass distribution continues to persist: the existence of a gap between the NS masses (ending around $2 M_{\odot}$) and BH masses (roughly $4 M_{\odot}$ and above)[70, 71]. However, bear in mind that the gap is statistical in nature and some BHs have error bars that fall within this gap, but even if this gap is not pristine, it is likely that there is a dearth of remnants with masses between $2 - 4 M_{\odot}$.

The distribution of remnant masses, along with theory predictions assuming rapid or delayed explosions, is shown in figure 7. The top panel shows the observed distribution (using the most-likely masses), clearly showing the observed mass gap. The bottom panel shows the number distribution for 3 different models: rapid explosion, delayed explosion, and former model used by the STARTRACK code[72]. Only the rapid explosion model produces a gap, suggesting that the turbulent engine must grow quickly. This result supports a Rayleigh-Taylor instability.

But this is not the end of the story. The current paradox with this gap is that if it truly exists, it argues against many supernovae with a large amount of fallback. The supernova energies produced by our two simplistic models at zero and solar metallicity are shown in figure 8. The rapid explosion model which produces a gap, does not produce any weak fallback supernovae. But such supernovae seem to exist[73]. How can we have weak supernovae but no fallback? Barring a theoretical misunderstanding (possible), one of the results, or more likely our interpretation of the results, is incorrect. Perhaps there are remnants with masses within the ‘‘gap’’ region, but they are sufficiently rare

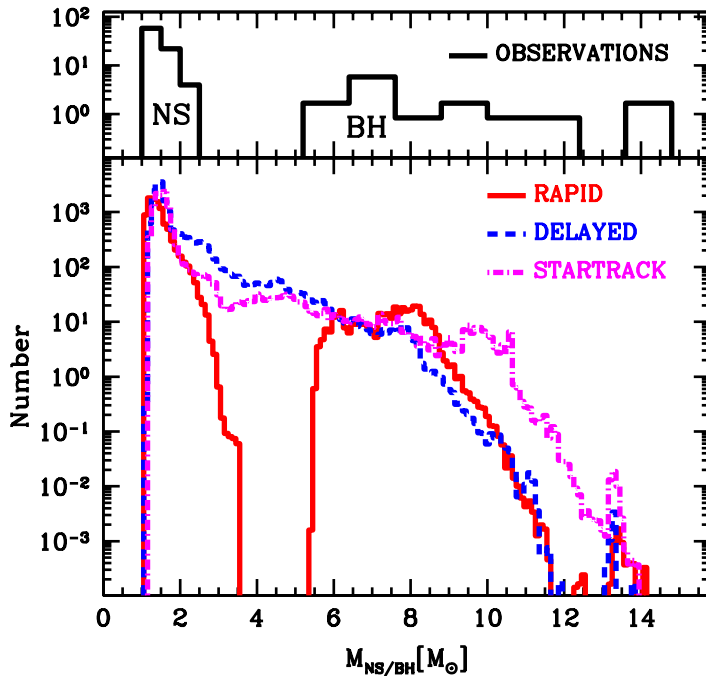


Figure 7. Neutron star/black hole mass distribution of the Galactic population of Roche lobe overflow and wind fed X-ray binaries (top) with the predicted rates for 3 different models: rapid, delayed, and old formalism used in STARTRACK[72]. Note that only the rapid explosion model produces the observed gap.

that they have yet to be observed (requiring a bigger sample). This would allow some weak supernovae.

The primary difficulty in using the compact remnant masses to constrain the supernova engine is the small sample statistics and potentially biased data of the X-ray binary population. Gravitational waves, with the potential to double the number of systems in a few years, can provide new insight into the compact remnant distribution. Unfortunately, although gravitational waves accurately measure the chirp mass, it is much more difficult to calculate the component star masses[74]. Figure 9 shows the range of possible inferred masses for a series of binary mass pairs (4 different chirp masses). As with our X-ray binary systems, we will have to use large-sample statistics to demonstrate a “gap” in the compact remnant masses. Unfortunately, gravitational

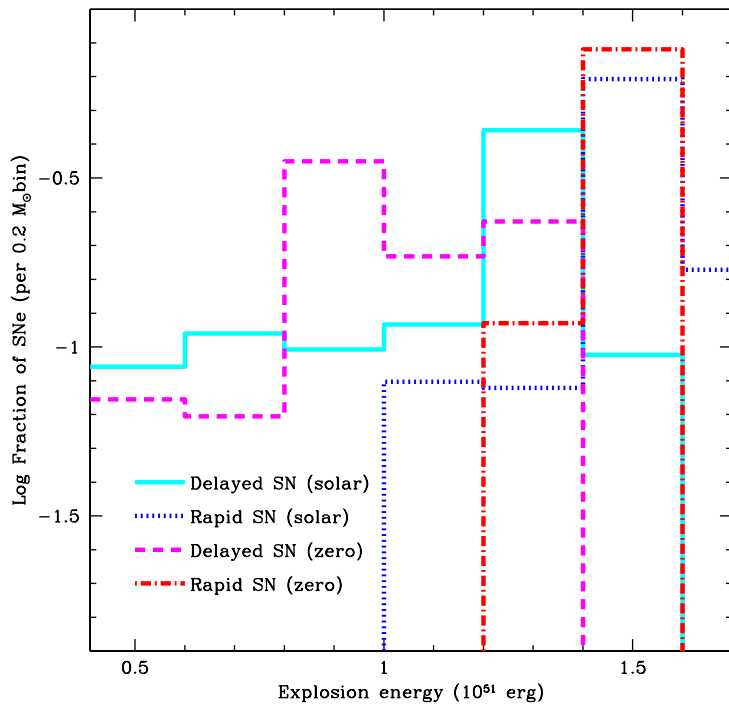


Figure 8. Distribution of supernova explosion energy for our delayed and rapid explosions at two metallicities (solar and zero metallicity). The rapid explosion mechanism produces only explosions in the 1-2foe energy range, whereas the delayed mechanism produces a wide range of supernova explosion energies. The narrow range in the rapid explosion is why it can produce a gap: either it produces a strong explosion or it fails to make an explosion. Delayed engines produce much more fallback, filling in the gap.

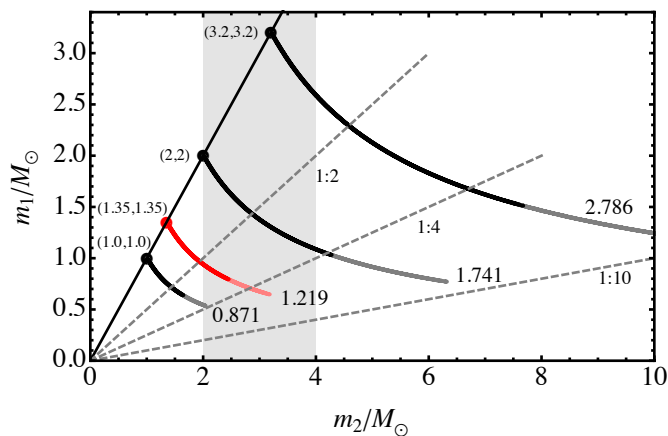


Figure 9. 90% confidence regions for a number of different non-spinning compact-binary configurations. The number at the end of each confidence region is the chirp mass of the binary. The gray shaded region indicates the current observational mass gap[74]. Because gravitational waves do not measure the component masses, it is difficult to constrain component masses to better than 10-30%.

wave observations are limited to binary systems. Although it is likely that gravitational waves will determine whether the gap truly exists, it will be difficult to determine whether this gap only exists in binary systems.

In X-ray binaries and binary compact mergers (gravitational wave detections), the inferred BH mass is the mass of the BH at formation plus the additional mass accreted in the binary. Measurements of solitary BHs will provide a more direct measurement of the BH mass distribution at formation. In addition, binary systems may be a biased set (e.g., BHs that receive strong kicks, perhaps the lowest mass BH systems, have a lower probability of remaining bound). The biases in BH binary formation are not well understood. A Hubble Space Telescope program is ongoing to look for single BHs using microlensing. WFIRST has the potential to do these studies and increase our understanding of single BH masses.

The connection between supernovae and compact remnants places us in an ideal position to use observations of one to constrain the other. The next decade should bring about many new discoveries in these fields.

References

- [1] Colgate S. A., White R. H. 1966, *ApJ*, 143, 626
- [2] Herant, M., Benz, W., Hix, W. R., Fryer, C. L., Colgate S. A. 1994, *ApJ*, 435, 339
- [3] Houck, J. C. and Chevalier, R. A. 1991, *ApJ*, 376, 234
- [4] Fryer, C. L., Benz, W., Herant, M. 1996, *ApJ*, 460, 801
- [5] Bethe, H. A., *Rev. Mod. Phys.*, 62, 801
- [6] Fryer, C. L. and Young, P. A. 2007, *ApJ*, 659, 1438
- [7] Houck, J. C. and Chevalier, R. A. 1992, *ApJ*, 395, 592
- [8] Blondin, J. M., Mezzacappa, A. and DeMarino, C. 2003, *ApJ*, 584, 971
- [9] Blondin, J. M. and Mezzacappa, A. 2006, *ApJ*, 642, 401
- [10] Miller, D. S., Wilson, J. R., Mayler, R. W. 1993, *ApJ*, 415, 278
- [11] Colgate, S. A., Herant, M., & Benz, W. 2003, *Phys. Rep.* 227, 157
- [12] Endal, A.S., and Sofia, S. 1978, *ApJ*, 220, 279
- [13] Fryer, C.L., and Heger, A. 2000, *ApJ*, 541, 1033
- [14] Keil, W., Janka, H.-T., and Müller, E. 1996, *ApJ*, 473, L111
- [15] Dessart, L., Burrows, A., Livne, E., Ott, C.D. 2006, *ApJ*, 645, 534
- [16] Foglizzo, T., Galletti, P., Scheck, L., & Janka, H.-T. 2007, *ApJ*, 654, 1006
- [17] Zwicky, F. 1938, *ApJ*, 88, 522
- [18] Burrows, A., Livne, E., Dessart, L., Ott, C. D., Murphy, J. 2006, *New Astronomy*, 50, 487
- [19] Yoshida, S., Ohnishi, N., Yamada, S. 2007, *ApJ*, 665, 1268
- [20] Akiyama, S., Wheeler, J.C., Meier, D.L., Lichtenstadt, I. 2003, *ApJ*, 584, 954
- [21] Wheeler, J.C., Akiyama, S., & Williams, P.T. 2005, *Ap&SS*, 298, 3
- [22] Dessart, L., Burrows, A., Livne, E., Ott, C.D. 2008, *ApJ*, 673, L43
- [23] Colgate, S. A. 1971, *ApJ*, 163, 221
- [24] Woosley, S. E. 1989, *NY Acad. Sci. Ann.*, 571, 397
- [25] MacFadyen, A. I., Woosley, S. E., Heger, A. 2001, *ApJ*, 550, 410
- [26] Young, P. A. 2007, *ApJ*, 664, 1033
- [27] Zhang, W., Woosley, S. E., Heger, A. 2008, *ApJ*, 679, 639
- [28] Ugliano, M., Janka, H.-T., Marek, A., & Arcones, A. 2012, *ApJ*, 757, 69
- [29] Dexter, J., & Kasen, D. 2013, *ApJ*, 772, 30
- [30] Fryer, C. L. 2009, *ApJ*, 699, 409

- [31] Woosley, S. E. 1993, *ApJ*, 405, 273
- [32] Popham, R., Woosley, S. E., Fryer, C. L. 1999, 518, 356
- [33] Barkat, Z., Rakavy, G., & Sack, N. 1967, *Phys. Rev. Lett.*, 18, 379
- [34] Woosley, S. E., & Weaver, T. A. 1982, in *Supernovae: A Survey of Current Research*, ed. M. J. Rees & R. J. Stoneham (Dordrecht: Reidel), 79
- [35] Bond, J. R., Arnett, W. D., & Carr, B. J. 1984, *ApJ*, 280, 825
- [36] Carr, B. J., Bond, J. R., & Arnett, W. D. 1984, *ApJ*, 277, 445
- [37] Fryer, C. L., Woosley, S. E., & Heger, A. 2001, *ApJ*, 550, 372
- [38] Fryer, C. L., & Heger, A. 2011, *Astron. Nachrichten*, 332, 408
- [39] Fryer, C. L., Belczynski, K., Wiktorowicz, G., Dominik, M., Kalogera, V., Holz, D. E. 2012, *ApJ*, 749, 91
- [40] Maeda, K., Tanaka, M., Nomoto, K., Tominaga, N., Kawabata, K., Mazzali, P. A., Umeda, H., Suzuki, T., Hattori, T. 2005, *ApJ*, 666, 1069
- [41] Bruenn, S. W., Mezzacappa, A., Hix, W. R., Blondin, J. M., Marronetti, P., Messer, O. E. B., Dirk, C. J., Yoshida, S., *astro-ph/1002.4914*
- [42] Ellinger, C. I., Rockefeller, G., Fryer, C. L., Young, P. A., Park, S., *astro-ph/1305.4137*
- [43] Fryer, C.L. 1999, *ApJ*, 522, 413
- [44] Heger, A., Fryer, C.L., Woosley, S.E., Langer, N., & Hartmann, D.H. *ApJ*, 591, 288
- [45] Fryer, C. L., & Kalogera, V. 1998, *ApJ*, 499, 520
- [46] Fryer, C. L., Burrows, A., & Benz, W. 1998, *ApJ*, 496, 333
- [47] Gualandris, A., Colpi, M., Zwart, S. P., & Possenti, A. 2005, *ApJ*, 618, 845
- [48] Willems, B., Henninger, M., Levin, T., Ivanova, N., Kalogera, V., McGhee, K., Timmes, F.X., & Fryer, C.L. 2005, *ApJ*, 625, 324
- [49] Fragos, t., Willems, B., Kalogera, V., Ivanova, N., Rockefeller, G., Fryer, C. L., & Young, P. A. 2009, *ApJ*, 697, 1057
- [50] Cordes, J. M., & Chernoff, D. F. 1998, *ApJ*, 505, 315
- [51] Arzoumanian, Z., Chernoff, D. F., & Cordes, J. M. 2002, *ApJ*, 568, 289
- [52] Gott, J. R. I., Gunn, J. E., & Ostriker, J. P. 1970, *ApJ*, 160, L91
- [53] Harrison, E. R., & Tademaru, E. 1975, *ApJ*, 201, 447
- [54] Fryer, C. L. 2004, *ApJ*, 601, L175
- [55] Herant, M. 1995, *Phys. Rep.*, 256, 117
- [56] Buras, R., Rampp, M., Janka, H.-T., & Kifonidis, K. 2003, *Phys. Rev. Lett.*, 90, 1101
- [57] Socrates, A., Blaes, O., Hungerford, A., Fryer, C. L. 2005, *ApJ*, 632, 531
- [58] Kusenko, A., & Segré, G. 1996, *Phys. Rev. Lett.* 77, 4872
- [59] Kusenko, A., & Segré, G. 1997, *Phys. Lett. B*, 396, 197
- [60] Barkovitch, M., D’Olivo, J.-C., Montemayor, R., & Zanella, J. F. 2002, *Phys. Rev. D.*, 66, 123005
- [61] Barkovitch, M., D’Olivo, J.-C., Montemayor, R., & Zanella, J. F. 2004, *Phys. Rev. D.*, 70, 043005
- [62] Fuller, G. M., Kusenko, A., Mocioiu, I., & Pascoli, S. 2003, *Phys. Rev. D*, 68, 103002
- [63] Kusenko, A. 2004, *Int. J. Mod. Phys. D* 2004, 13, 2005
- [64] Fryer, C. L., & Kusenko, A. 2005, *ApJ*, 163, 335
- [65] Whalen, D. J. & Fryer, C. L. 2012, *ApJ*, 756, L19
- [66] Thorsett, S. E. & Chakrabarty, D. 1999, *ApJ*, 512, 288
- [67] Bailyn, C. D., Jain, R. K., Coppi, P., Orosz, J. A. 1998, *ApJ*, 499, 367
- [68] van Kerkwijk, M.H., van paradijs, J., Zuiderwijk, E. J. 1995, *A&A*, 303, 497
- [69] Demorest, P.B., Penucci, T., Ransom, S. M., Roberts, M. S. E., & Hessles, J. W. T. 2010, *Nature*, 467, 1081
- [70] Ozel, F., Psaltis, D., Narayan, R., & McClintock, J. E. 2010, *ApJ*, 725, 1918
- [71] Farr, W. M., Sravan, N., & Cantrell, A. et al. 2011, *ApJ*, 741, 103
- [72] Belczynski, K., Wiktorowicz, G., Fryer, C. L., Holz, D. E., & Kalogera, V. 2012, *ApJ*, 757, 91
- [73] Moriya, T., Tominaga, N., Tanaka, M., Nomoto, K., Sauer, D. N., Mazzali, P. A., Maeda, K., Suzuki, T. 2010, *ApJ*, 719, 1445

- [74] Hannam, M., Brown, D. A., Fairhurst, S., Fryer, C. L., Harry, I. W. 2013, ApJ, 766, L14